Sequential activation of molecular and macroscopic spin-state switching within the hysteretic region following pulsed light excitation

Karl Ridier, William Nicolazzi, L. Salmon, Gábor Molnár, Azzedine Bousseksou

Sequential activation of molecular and macroscopic spin-state switching within the hysteretic region following pulsed light excitation

Karl Ridier, William Nicolazzi, Lionel Salmon, Gábor Molnár* and Azzedine Bousseksou**

Dr. K. Ridier, Dr. W. Nicolazzi, Dr. L. Salmon, Dr. G. Molnár, Dr. A. Bousseksou
Laboratoire de Chimie de Coordination, CNRS & Université de Toulouse
31077 Toulouse, France
E-mail: karl.ridier@lcc-toulouse.fr, gabor.molnar@lcc-toulouse.fr, azzedine.bousseksou@lcc-toulouse.fr

Keywords: photo-responsive materials, bistability, dynamics, spin crossover, pump-probe optical microscopy

Molecular spin-crossover (SCO) compounds constitute a promising class of photoactive materials exhibiting efficient photo-induced phase transitions (PIPTs), driven by cooperative elastic interactions between the switchable molecules. Taking advantage of the unique, picture-perfect reproducibility of the spin-transition properties in the compound [Fe(HB(1,2,4-triazol-1-yl)$_3$)$_2$], we have dissected the spatiotemporal dynamics of the PIPT within the thermodynamic metastability (hysteretic) region of a single crystal, using pump-probe optical microscopy. Beyond a threshold laser excitation density, complete PIPTs were evidenced, with conversion rates up to 200 switched molecules per absorbed photon. We show that the PIPT takes place through the sequential activation of two (molecular and macroscopic) switching mechanisms, occurring on sub-µs and ms timescales, governed by the intramolecular and the free energy barrier of the system, respectively. As a result, we find that the thermodynamic metastability has strictly no influence on the sub-ms switching dynamics. The latter can be described as a homogeneous molecular conversion process with linear response to laser excitation. Remarkably, in this regime, even a 100 % photo-conversion may not give rise to a PIPT. These results provide new insight on the intrinsic dynamical limits of the PIPT in SCO solids (and other types of bistable materials), which is an important issue, from a technological perspective, for achieving fast and efficient photo-control of the functionalities of condensed matter.

1. Introduction

The reversible transformation of the physical properties of condensed matter in response to short light irradiation is an important, emerging topic in materials science. Within this broad field, much attention has been focused on the investigation of photo-induced effects in systems showing strong cooperative phenomena, with the appealing perspective of achieving fast and efficient macroscopic phase transformations induced by light excitations. As such, the concept of photo-induced phase transitions (PIPTs) has emerged,[1] which refers to the large-scale structural and electronic changes in macroscopic solids – similar to a domino effect – triggered by a local photoexcitation process and driven by cooperative electron-lattice interactions between constituents. Such a highly cooperative (non-linear) photo-responsiveness has been reported in various systems, such as correlated oxides, π-conjugated polymers and charge-transfer compounds.[2–10]

Among these materials, molecular spin-crossover (SCO) complexes arguably constitute one of the most fascinating examples of photoactive materials. These coordination complexes can switch reversibly between the so-called low-spin (LS) and high-spin (HS) electronic configurations through the application of a variety of external stimuli,[11–13] including temperature change, light irradiation (from x-ray to visible range) and even electron irradiation. While the ultrafast electronic and molecular structural dynamics following the LS-to-HS photoswitching process – known as light-induced excited spin-state trapping (LIESST) effect[14] – has been scrutinized at the molecular level (mainly in solution) since several decades,[15–20] a series of recent studies have addressed the macroscopic response of SCO solids to (ultra-)short light pulses, combining time-resolved x-ray diffraction and pump-probe optical measurements.[21–27] These investigations revealed that the molecular photoswitching (LIESST) event, which always occurs through ultrafast (sub-picosecond) intersystem crossing, effectively triggers a multistep transformation of the material, characteristic of PIPTs, governed by the lattice dynamics. Indeed, as the spin-state switching is accompanied by a sizeable change of the

molecular volume, an intricate combination of short- and long-range elastic interactions (mediated through the lattice) exist between the SCO molecules,[28] at the origin of non-linear, cooperative switching phenomena. This elastically driven feedback between volume-changing molecules and lattice deformation, coupled to the transient increase of the lattice temperature, was found to induce self-amplified responses to light irradiation,[23,25] characterized by enhanced photoconversion yields and extended lifetimes of the photo-induced state.

More interestingly, in some 'highly cooperative' SCO materials, it is well known that the strong elastic intermolecular interactions can give rise to the formation of a macroscopic free energy barrier, which defines a region of thermodynamic metastability between the LS and HS phases – with virtually infinite lifetime – resulting in first-order spin transitions and associated hysteretic phenomena around room temperature.[29] Undoubtedly, applying a pulsed light irradiation within the hysteretic region appears as the most promising way to induce highly efficient PIPTs, since the switching process takes place from a metastable (LS or HS) to a thermodynamically stable state. Although PIPTs induced by pulsed laser excitations inside the hysteretic region have already been reported for several SCO compounds[30–39] as well as for some closely related compounds,[2,40,41] the mechanistic details of this laser-induced switching process have never been elucidated.[29]

Unfortunately, the switching dynamics within the hysteretic region is, in principle, not accessible by conventional pump-probe experiments, merely because the sample does not recover its initial state after the switching event, due to the long lifetime of the photoinduced state. This issue, coupled to the frequently observed fatigability of SCO solids upon repeated switching cycles, has basically restricted the scope of possible investigations to (challenging) single-shot experiments.[34,37]

In this study, we have followed an alternative strategy. The recent discovery of an exceptionally high spin-state switching endurance (>10^7 cycles[42]) in the molecular SCO complex [Fe(HB(1,2,4-triazol-1-yl)$_3$)$_2$] (**1**), especially within the hysteretic region,[43] allowed us to

remove these experimental bottlenecks. Indeed, these unprecedented features enable the same crystal to be prepared repeatedly in the same initial state after each laser pulse by thermal cycling, making it possible to perform reliable, quantitative pump-probe measurements within the thermal hysteresis loop of a unique single crystal. This way, we have investigated the spatiotemporal dynamics of the photoswitching process, triggered by a nanosecond laser pulse, using time-resolved pump-probe optical microscopy with µs temporal and µm spatial resolution. Based on this approach, in this paper, we intended to address the following questions: (i) What are the successive steps involved in the photo-transformation pathway of a SCO single crystal, from one long-lived spin state to the other, within the hysteretic region? (ii) What is the pertinent timescale for this macroscopic photoswitching process? and (iii) What is the achievable amplification rate originating from the thermodynamic metastability?

2. Results and Discussion

Single crystals of (**1**) exhibit a first-order, isostructural spin transition above room temperature (ca. 61 °C) between the low-temperature LS (S = 0) and high-temperature HS (S = 2) phases.[44] Figure 1a shows the typical thermal hysteresis loop of a crystal of (**1**) (ca. 50 × 50 × 15 µm^3 size) obtained by measuring the temperature dependence of the optical transmission (λ = 540-570 nm) through the sample. As shown in our previous work performed under similar experimental conditions,[43,45] crystals of (**1**) display a well-defined, quasi-static hysteresis loop, with no notable kinetic effects (i.e., metastable sates with very long lifetime) and extremely abrupt spin transitions at $T^{\uparrow}$ = 61.09 °C and $T^{\downarrow}$ = 60.12 °C. Note that the measurement of the optical transmission over a wide temperature range [20–120 °C] reveals that the hysteretic, first-order transition does not occur between full LS and HS states (see Figure S1 in the Supporting Information), but rather between macroscopic states with $n_{HS} \approx 0.12$ and 0.70, hereafter denoted LS_1 and HS_1, respectively. In the following, the fraction of switched molecules within the thermal hysteresis loop will be referred as $\Delta n_1 = [I - I_{LS_1}]/[I_{HS_1} - I_{LS_1}]$, where I_{LS_1} and I_{HS_1}

are the optical transmission intensities measured in the LS_1 and HS_1 state, respectively. Importantly, no minor hysteresis loop is observed in single crystals of (**1**), as only the LS_1 and HS_1 states are accessible in quasi-static conditions.

We have carried out a series of time-resolved optical microscopy measurements to probe the spatiotemporal dynamics of the photoswitching process, induced by a 4-ns laser pulse (at λ_{laser} = 532 nm, i.e. within the ligand-field absorption band of the complex in the LS state, see Figure S2), by varying the temperature of the crystal (within the thermal hysteresis loop) and the laser excitation energy density (from 0 to 90 mJ cm^{-2}). The Gaussian laser beam was focused on the crystal to a spot with a diameter of ca. 125 µm, enabling a closely homogeneous sample excitation. Within the hysteretic region, our measurements demonstrate that the pulsed light irradiation of the crystal (initially prepared in the LS_1 state) above a certain threshold excitation density induces its complete conversion into the steady macroscopic HS_1 state. Figure 1b shows the typical evolution of this threshold excitation density, E_{th}, at various temperatures within the hysteresis loop of the crystal. As the temperature decreases from $T^{\uparrow}$, E_{th} grows linearly, but shows a sizeable jump around T_{eq} = 60.65 °C, close to the barycenter of the thermal hysteresis ($T^{\uparrow} + T^{\downarrow}$) / 2. This leap of E_{th} indicates a change in the thermodynamic phase stability of the crystal. Hence, T_{eq} can be assimilated to the thermodynamic equilibrium temperature between the macroscopic LS_1 and HS_1 phases. Consequently, two distinct regions can be considered within the thermal hysteresis loop: for $T > T_{eq}$ the LS_1 (resp. HS_1) state is the thermodynamically metastable (resp. stable) state, and contrariwise for $T < T_{eq}$. These considerations can be illustrated using the well-established thermodynamic model for cooperative SCO materials,[46] which provides a clear picture of the double-well form of the Gibbs free energy of the system in the two regions of the thermal hysteresis loop (see Figure 1c and S3). As such, for $T > T_{eq}$, it appears that the free energy difference between the two phases involves the existence of a thermodynamic driving force, which favors the photo-conversion process of the system into the final HS_1 state. Conversely, as the HS_1 state is metastable for $T < T_{eq}$, the thermodynamic

potential acts as an antagonistic force in the photo-induced LS-to-HS conversion, resulting in the observed increase of E_{th}.

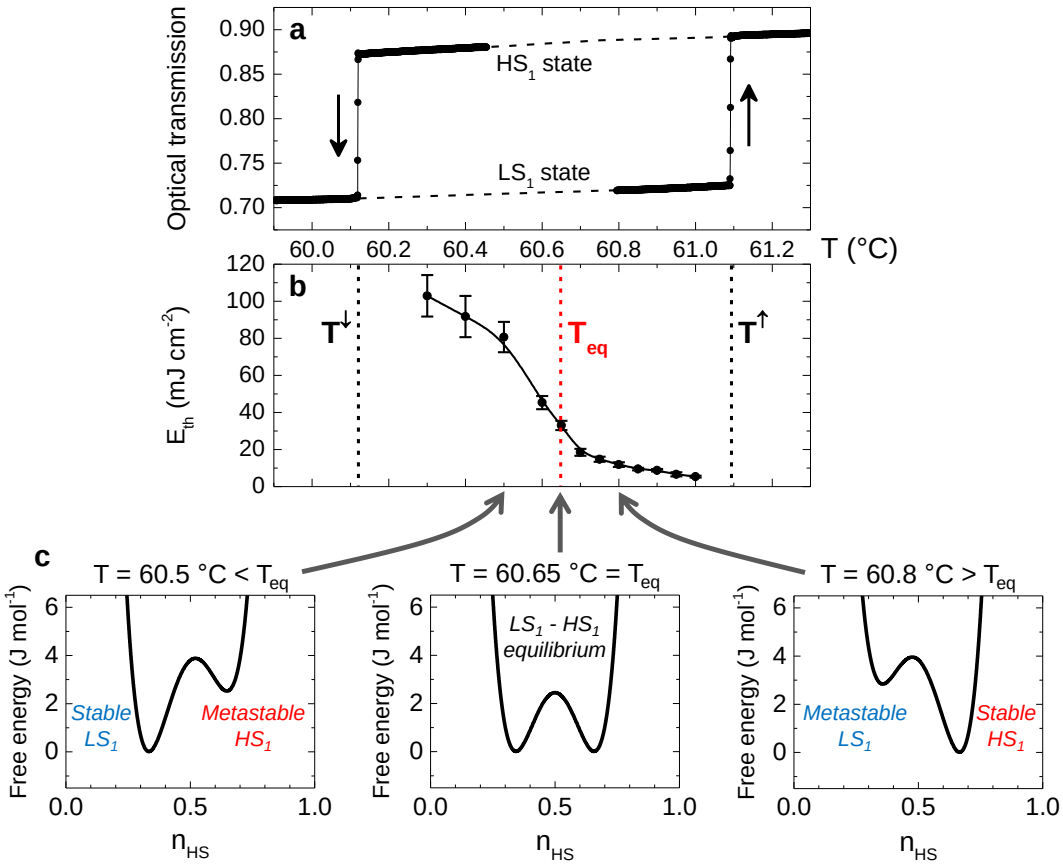

Figure 1. Thermal hysteresis loop and thermodynamic properties of the crystals of (1). (a) Temperature dependence of the optical transmission $T = I / I_0$ (λ = 540-570 nm) through a single crystal of (**1**) showing a 1-°C-wide, quasi-static thermal hysteresis loop between the LS_1 and HS_1 phases. The arrows indicate the direction of heating and cooling (±1 °C/min). (b) Evolution of the threshold excitation density E_{th} as a function of the temperature within the thermal hysteresis loop. E_{th} refers to the minimum laser energy density required to achieve the complete transformation of the crystal (initially prepared in the LS_1 state) into the steady macroscopic HS_1 state. The error bars indicate the experimental uncertainty on the excitation density value. (c) Typical forms of the Gibbs free energy of the system at $T = T_{eq}$ and in the two regions of the thermal hysteresis loop at T = 60.5 and 60.8 °C (on both sides of T_{eq}), calculated using a thermodynamic approach based on binary mixture model solved in the framework of the mean-field approximation.

In the following, combining real-time and pump-probe optical microscopy measurements (see the Experimental Section and Figure S4), we have carried out a detailed investigation of the out-of-equilibrium spatiotemporal dynamics of the pulsed-laser-induced spin transition in the two regions of the thermal hysteresis loop (on both sides of T_{eq}). As an example, Figure 2a and

2b display selected optical microscopy snapshots of the crystal (initially prepared in the LS_1 state), showing the relative change of the optical transmission $(I - I_{t=0}) / I_{t=0}$ following the application (at $t = 0$) of a laser pulse at $T = 60.8$ °C > T_{eq} ($E = 36$ mJ cm^{-2}) and $T = 60.5$ °C < T_{eq} ($E = 49$ mJ cm^{-2}), respectively. (Figure S5 and S6 display a more compete series of images recorded for various laser excitation densities at the two temperatures studied.) The variation of the optical intensity measured in transmission allows to monitor the spatiotemporal evolution of the fraction of photoswitched HS molecules, Δn_1. Based on these time-resolved optical microscopy data, Figure 2c and 2d depict the temporal evolution of Δn_1 within the whole crystal, following a laser excitation of different energy densities, at $T = 60.8$ °C > T_{eq} (stable HS_1 state) and $T = 60.5$ °C < T_{eq} (stable LS_1 state), respectively. Overall, these measurements reveal the existence of (at least) two different switching mechanisms in response to the nanosecond laser pulse. Basically, we observe that the fraction of photoswitched molecules has already reached a plateau in the µs–ms time domain (which is linear with the excitation energy density, see Figure 2e), indicating the existence of a sub-µs switching dynamics (faster than the current temporal resolution of our pump-probe measurements). Then, in the ms–s time domain, the activation of strongly non-linear, cooperative phenomena is clearly evidenced, resulting in either a relaxation of the crystal in the initial LS_1 state or its complete conversion in the HS_1 state (Figure 2f).

Numerous studies allowed to elucidate the out-of-equilibrium mechanisms of the laser-induced spin transition in SCO solids with a sub-µs temporal resolution.[21–26] Notably, femtosecond optical spectroscopic measurements were recently performed by us on thin films of (**1**).[27] First, absorption of light at the molecular level locally switches a small fraction of molecules, $\Delta n^{h\nu}$, from the LS to the HS state, through ultrafast (< ps) intersystem crossing.[17] Considering the absorption coefficient of the crystals of (**1**) in the LS_1 state at the excitation wavelength ($\alpha \approx 200$ cm^{-1}) and a quantum efficiency equal to unity,[47] the expected fraction of photoswitched HS molecules is $\Delta n^{h\nu} < 2.3$ % in the laser energy density range used in this work. This value is

in line with the photoinduced HS fraction measured in thin films of (**1**) on the sub-ps timescale, using comparable excitation densities.[27] Following this early photoswitching step, a second molecular conversion process (hereafter denoted Δn^{th}) is expected to occur on a timescale of tens of nanoseconds, associated with the thermal activation of the intramolecular LS ↔ HS energy barrier.[27] This delayed thermally activated amplification of the HS fraction is known to be mainly driven by thermoelastic effects, i.e., in response to the volume expansion of the crystal lattice[25,26] and, predominantly, due to the transient increase of the crystal temperature, as a large part of the absorbed photon energy is converted to heat.[27,34,35] Knowing the specific heat capacity of (**1**) at 60 °C (C_p = 1107 J kg^{-1} K^{-1}),[48] a basic calculation indicates that the global increase of the crystal temperature can be estimated of the order of 10 °C for the highest excitation energy densities used. Note that the large laser penetration depth ($\delta \approx$ 50 µm at λ_{laser} = 532 nm) compared with the crystal thickness (≈ 15 µm), shall result in a fairly uniform distribution of photo-switched molecules, and then a homogeneous transient heating within the crystal.

The fraction of photoinduced HS molecules observed in our pump-probe experiments in the microsecond time domain is presumably the result of the two successive switching processes described above. These two fast (sub-µs) conversion phenomena are inaccessible with the current temporal resolution of our pump-probe setup. Remarkably, as shown in Figure 2e, the fraction of photoswitched molecules measured at t = 5 µs grows linearly with the laser excitation density, and in an identical way for the two temperatures T = 60.5 and 60.8 °C (i.e., in both regions of the hysteresis loop). This key observation signifies that the thermodynamic metastability has no effect on the photoresponse of the crystal on such a short timescale. Instead, further measurements performed at constant laser excitation density (Figure S7) show a strong temperature dependence of the photo-induced HS fraction on the µs timescale, which corroborates the thermally activated character of the switching process. In addition, the optical microscopy images, recorded on the µs–ms timescale, show that the photoswitched molecules

are homogeneously distributed in the crystal (Figure 2a and 2b). These different observations thus support the occurrence of a purely molecular switching process on the sub-µs timescale, mainly driven by transient photo-thermal effects. Interestingly, contrary to our previous observations made in the thin films of (**1**),[27] this thermally activated amplification of the HS fraction varies linearly (no threshold effect) with the laser excitation density. This linear trend can arise from the fact that the spin-state switching within the hysteresis loop accounts for only ≈ 58 % of the full spin transition (between n_{HS} = 0.12 and 0.70), in a range where we can assume that the thermal dependence of the HS fraction approaches a linear behavior. Moreover, in thin films, this thermally driven amplification was also in competition with the heat dissipation process into the external environment, the latter taking place on the same timescale (≈ 10-100 ns).[27] This competition effect does not exist in single crystals (the heat dissipation instead occurring on the millisecond timescale, vide infra), which corroborates the linear behavior of the HS fraction with the laser excitation density.

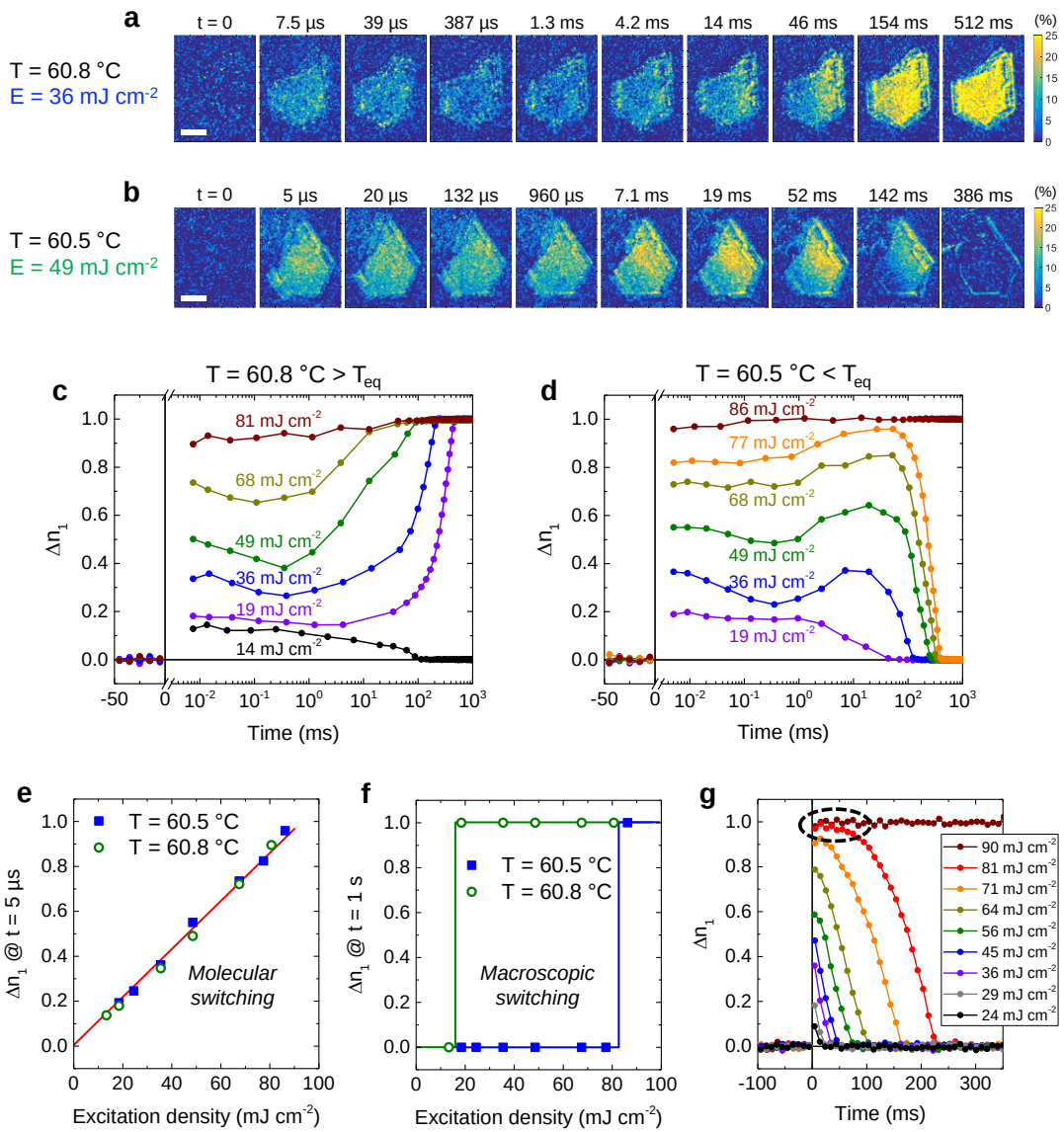

Figure 2. Photoresponse of a single crystal of (1) to a nanosecond laser pulse within the hysteretic region. (a and b) Selected optical microscopy snapshots of the crystal (initially prepared in the LS_1 state) during the laser-induced spin transition at (a) T = 60.8 °C (E = 36 mJ cm^{-2}) and (b) T = 60.5 °C (E = 49 mJ cm^{-2}). The laser pulse was applied at t = 0. The snapshots correspond to the $(I - I_{t=0}) / I_{t=0}$ images, where I and $I_{t=0}$ are the optical transmission images of the crystal measured at times t and t = 0, respectively. The complete conversion into the HS_1 state (Δn_1 = 1) corresponds to a relative variation $(I - I_{t=0}) / I_{t=0}$ of 24 %. Scale bars, 20 µm. (c and d) Time evolution of the fraction of photoswitched HS molecules, Δn_1, following a laser pulse with various energy densities, at two different temperatures within the thermal hysteresis loop (c) T = 60.8 °C (thermodynamically stable HS_1 state) and (d) T = 60.5 °C (thermodynamically stable LS_1 state). (e and f) Evolution of Δn_1 measured at (e) t = 5 µs and (f) t = 1 s with respect to the laser excitation density for the two temperatures studied (60.5 and 60.8 °C). (g) Time evolution of Δn_1 following a laser pulse with various excitation energy densities at T = 60.5 °C measured in real time. Close to the threshold excitation density (E = 81 mJ cm^{-2} < E_{th}), a complete conversion of the molecules in the HS state is observed (encircled), followed by a relaxation of the crystal in the initial LS_1 state.

2.1. In the thermodynamically stable HS_1 state regime

As shown in Figure 2c, the measurements carried out at T = 60.8 °C (stable HS_1 state) strikingly reveal the threshold effect on the laser excitation density to induce the complete LS_1-to-HS_1 conversion of the crystal. Below this threshold density (E = 14 mJ cm^{-2} < E_{th}), the fraction of photo-switched molecules follows a plateau ($\Delta n_1^{th} \approx 0.12$) on the 5 µs – 10 ms time domain, before relaxing back to the initial LS_1 state at t = 100 ms. For a slightly higher excitation density (E = 19 mJ cm^{-2} > E_{th}), Δn_1^{th} is just high enough (0.17) to trigger the transformation of the entire crystal, completed at t = 500 ms. The spatiotemporal mechanisms of this photo-conversion process are clearly depicted on the optical microscopy images (see Figure 2a and S5 for the various excitation energy densities used). As an example, for an excitation density of E = 36 mJ cm^{-2} (Figure 2a), while the photoinduced HS molecules appear to be homogeneously distributed within the sample on the µs–ms timescale, the heterogeneous nucleation of the HS_1 phase is observed on the right edge of the crystal at ca. t = 14 ms, followed by the growth of this newly-formed domain, via the propagation of a LS-HS phase boundary, until the complete transformation of the crystal. As shown in Figure S8, the detailed analysis of the time evolution of the photoinduced HS fraction in two selected areas of the sample (at both ends of the crystal) clearly reveals the existence of a crossover (around t = 1–10 ms) between a "homogeneous" regime and a regime where the heterogeneities are strongly accentuated. It is well known that the thermodynamic metastability implies that the macroscopic spin-state switching takes place via a phase separation (nucleation and growth) process, the driving force of the domain formation and phase-boundary propagation being the thermodynamic instability (i.e., the free energy difference) between the two phases.[29] However, the most conspicuous observation is that the activation of this thermodynamic driving force, governed by the macroscopic free energy barrier, typically occurs on the 1–10 ms timescale. The existence of a threshold excitation energy to induce the complete transformation of the crystal is a typical characteristic of first-order phase transition.[49] Indeed, phase separation has an energy cost (interfacial and

elastic energy),[29] which will balance the thermodynamic driving force until a critical nucleus size is reached (i.e., a threshold laser excitation density).[36]

Interestingly, our measurements also show that the transition within the hysteretic region, from the metastable to the stable state, can reach extremely high yields using only moderate laser excitation energies. Typically, at 60.8 °C, the laser pulse of 19 mJ cm^{-2} (corresponding to a calculated photoswitched fraction of $\Delta n_1^{hv} \approx 0.5$ %) induces the thermally activated conversion of Δn_1^{th} = 17 % of the bulk material, which turns out to be sufficient to trigger the thermodynamically driven amplification process to attain the full HS_1 state. In this case, the conversion efficiency thus reaches ca. 34 switched molecules for one single photon for the photothermal conversion and ca. 200 switched molecules for the complete macroscopic transformation process. At high excitation density (E = 81 mJ cm^{-2}), our pump-probe optical measurements reveal that almost all molecules are thermally converted on the microsecond timescale. Even if virtually all molecules are converted at an early stage, the question arises, in this particular case, about the time it takes for the crystal to reach the HS_1 state (i.e., the thermodynamic equilibrium), since the macroscopic phase separation process is presumably not yet activated on such a short timescale. As the molecules are already in the HS state at such high excitation densities, the recovery of the thermodynamic equilibrium (and the hypothetic nucleation and growth process) would solely refer to a structural reorganization, which is not discernible in our optical microscopy experiments. Time-resolved structural measurements (e.g. x-ray diffraction) will be thus necessary to further explore the transformation pathway at such high excitation densities.

2.2. In the thermodynamically stable LS_1 state regime

As shown in Figure 1b and 2d, the threshold excitation density required to reach the steady macroscopic HS_1 state at T = 60.5 °C becomes significantly higher ($E_{th} \approx 80$ mJ cm^{-2}), because the final HS_1 state is now metastable. For energy densities $E < E_{th}$, as the laser excitation is not sufficient to overcome the thermodynamic energy barrier, a certain fraction of molecules is

transiently photo-converted before relaxing back into the LS state. As shown in Figure 2b and S6, a homogeneous photoswitching process is observed on the µs–ms timescale (within the limit of homogeneity of the Gaussian laser beam and the crystal itself), followed by a heterogeneous (phase separation) relaxation mechanism, completed within 100–500 ms. Interestingly, heterogeneities begin to appear around t = 1–10 ms (see Figure S8), with the formation of both LS and HS domains on the left and right parts of the crystal, respectively, the relaxation then taking place via the growth of the newly formed LS domain. It is worth mentioning that, for intermediate excitation densities, slight variations of Δn_1 are observed (a decrease followed by a small rise), before the complete relaxation (Figure 2d). These variations remain to be fully understood, but they might possibly arise from a competition between the elastic forces exerted by the LS lattice on the photoswitched HS molecules (which tend to push them back into the LS state)[25,26] and the concomitant formation and growth of a HS domain (stabilized by the transient increase of the crystal temperature). However, these phenomena should be also affected by the not perfectly homogeneous photoexcitation of the crystal.

Importantly, for laser excitations close to the threshold energy density (E = 77 mJ cm^{-2} < E_{th}), we observe that the relaxation into the LS_1 state takes place even though the fraction of photoswitched molecules Δn_1 has virtually reached 100 %. This remarkable evolution of Δn_1 was even better evidenced through real-time measurements (see Figure 2g), which turned out to be more suitable (compared to pump-probe techniques) to investigate such fine details. The striking observation here is that, in the stable LS_1 state region of the hysteresis (T < T_{eq}), there exists a range of laser excitation densities, which makes it possible to transiently switch ALL the molecules into the HS state (via a thermally activated molecular process), but which turns out to be insufficient to reach the macroscopic metastable HS_1 state (i.e., to surpass the thermodynamic energy barrier). Instead, the crystal remains in an out-of-equilibrium state – from a thermodynamic point of view – which ultimately leads to its complete relaxation into

the stable state. These results clearly evidence the existence of two decoupled conversion phenomena, each having their own activation energy and kinetics.

Note that the characteristic time associated with heat diffusion across the crystal, approximated by the ratio $\tau = L^2 / D_T \approx 1–10$ ms, where L is the characteristic size of the crystal and $D_T = 2.6 \times 10^{-7}$ m^2 s^{-1} is the thermal diffusivity,[43] gives the typical timescale for the recovery of the thermal equilibrium with the external environment. This confirms that the relaxation of the crystal (via the nucleation and growth process), which is completed within 100–500 ms, is not driven by the existence of temperature gradients within the sample. In fact, the recovery of the thermodynamic equilibrium appears to be limited by the growth kinetics of the macroscopic phase, i.e., the (slow) propagation velocity of the LS/HS phase boundary.[29]

3. Conclusion

In summary, by taking advantage of the outstanding properties of the molecular SCO compound [Fe(HB(1,2,4-triazol-1-yl)$_3$)$_2$] in terms of resilience and switching endurance (ca. 10,000 switches in the hysteresis loop endured in the present study while preserving <0.05 °C accuracy of the switching temperatures), we quantitatively assessed the spatiotemporal dynamics of the spin-transition process, induced by a pulsed laser excitation, within the thermodynamic metastability domain of a unique single crystal. We demonstrate that the photo-transformation pathway (and the subsequent switching dynamics) of SCO solids is singularly altered in the hysteretic region due to the existence of the thermodynamic energy barrier between the macroscopic phases, whose origin comes from the long-range elastic interactions between molecules. Our experiments, performed at two different temperatures within the thermal hysteresis loop – T = 60.5 and 60.8 °C, i.e., ±0.15 °C on both sides of T_{eq} – reveal the sequential activation of two different switching mechanisms, taking place on well distinct timescales and obeying very specific spatiotemporal dynamics. Specifically, we find that the primary photoswitching event (known to occur on the sub-ps timescale) is followed by a rapid (sub-µs),

homogeneous, molecular switching process, governed by the LS ↔ HS energy barrier at the molecular level, as it was already shown by us in a previous study.[27] Interestingly, the photoresponse of the crystal is found to be linear with the laser intensity, and identical for the two temperatures studied, revealing that the thermodynamic metastability does not intervene on this short 'molecular switching timescale'. Then, from t = 1–10 ms after the laser pulse, a novel regime is clearly identified with the activation of a nonlinear, cooperatively driven macroscopic conversion process, characterized by the nucleation and growth of domains. From this millisecond timescale, the response of the crystal shows drastic differences in the two regions of the thermal hysteresis loop, revealing that the effect of the metastable thermodynamic potential is now dominating the transformation dynamics of the solid. We postulate here that this regime change defines a 'phase-separation timescale', which corresponds to the typical activation time of the cooperatively driven phase transition, governed by the free energy barrier separating the two macroscopic phases. In our previous study carried out on thin films of the same compound,[27] we demonstrated the prominent role of the intramolecular LS-HS energy barrier, which was found to be the main bottleneck in the transition dynamics, limiting the thermally activated molecular switching dynamics around a few tens of nanoseconds. Analogously, in the present study, we demonstrate that the thermodynamic energy barrier within the metastability region of SCO solids, makes the macroscopic nucleation and growth process "frozen" on the sub-ms timescale, thus considerably limiting the dynamics of PIPTs. As a consequence of this double-dynamics photoswitching process, we show, in the stable LS_1 state region of the hysteresis ($T < T_{eq}$), that even a 100 % photo-thermal conversion of the molecules in the HS state may not give rise to a PIPT. In the stable HS_1 state region ($T > T_{eq}$), our observations reveal that the thermodynamic metastability enables strong amplification and extremely high light pulse-induced conversion yields to be achieved (up to 200 switched molecules for one single photon for the complete PIPT). In this case, the price to pay, however,

is that this thermodynamically driven amplification brings into severe restraints on the accessible switching rates between the macroscopic LS and HS phases.

An important perspective towards the aim of achieving fast and efficient photo-transformation will be the investigation of size reduction effects on the thermodynamically driven conversion phenomenon, which should be considerably accelerated at the nanometric scale. The study of the dynamical properties of the spin-state switching process within the hysteretic region of SCO nano-objects[13,50] remains the ultimate experimental challenge. In this context, the use of scanning probe microscopy methods opens up interesting perspectives,[51–53] even if reaching high temporal resolution remains a considerable defy. By analogy to superparamagnetism, it is possible that, below a certain critical size, the nano-object behaves as a single entity in which all SCO molecules switch coherently, without activation of the heterogeneous nucleation and growth process. This assumption appears as the most promising route to achieve fast and efficient laser pulse-induced transformation of the physical properties of molecular systems between two different long-lived phases around room temperature.

4. Experimental Section

Single crystals of (**1**) were synthesized in their solvent-free form as described previously.[44] They were enclosed in a variable-temperature microscope stage (Linkam Scientific Instruments, THMS350V), allowing the crystal temperature to be controlled with a precision of 0.01 °C. Bright-field optical microscopy images of the crystal were recorded in transmission mode using a ×50 magnification objective (numerical aperture, NA = 0.45). The sample was illuminated by a halogen lamp, but the probe spectral range was reduced to λ = 540-570 nm using a band-pass filter. The fraction of molecules in the HS state, $n_{HS}(x,t)$, was monitored through the spatiotemporal variation of the optical intensity $I(x,t)$ measured in transmission: $n_{HS}(x,t) = [I(x,t) - I_{LS}(x)] / [I_{HS}(x) - I_{LS}(x)]$, where $I_{HS}(x)$ and $I_{LS}(x)$ refer to the optical intensity at point x in the HS and LS states, respectively. The crystals were excited using a frequency-doubled Nd:YAG

laser emitting 4 ns pulses at λ_{laser} = 532 nm – falling into the (weak) ligand-field absorption band of the complex in the LS state (Figure S2). The Gaussian laser beam was focused on the crystal to a spot with a diameter (1/e^2 width) of $\varnothing \approx$ 125 µm, enabling a closely homogeneous sample excitation. The laser excitation density was adjusted between 0 and 90 mJ cm^{-2} using a variable optical density wheel. The laser light was filtered out using a notch filter (λ_{notch} = 532 nm) installed in front of the cameras. Time-resolved images were acquired either in real time using a CCD camera (Andor Technology Clara, 1392 × 1040 pixels of 6.45 µm size) or in a pump-probe approach using a gated Intensified-CCD camera (Andor Technology iStar DH734, 1024 × 1024 pixels of 13 µm size), synchronized with the laser pulses. The real-time images were recorded with a frame rate of 40 Hz (i.e., a time resolution of 25 ms), whereas the pump-probe setup allowed us to reach a time resolution of 5 µs. Indeed, using our optical imaging system, it turns out that the signal-to-noise ratio becomes too low on the sub-microsecond timescale due to a limited optical contrast between the LS and HS states in the probed spectral range. (N.B. Further improvement would be possible using UV light.) The combination of these two approaches makes it possible to obtain the spatiotemporal evolution of the fraction of photoswitched HS molecules $\Delta n_1(x,t)$ on the full time domain [5 µs – 1 s] (see Figure S4). Depending on the temperature and the laser energy density, the photoexcitation within the thermal hysteresis loop was followed either by a complete relaxation of the crystal into the initial LS_1 state, or a full conversion into the (meta-)stable HS_1 state. In the first case, the pump-probe experiments were carried out with a 1 Hz pump repetition rate. In the second case, the crystal was brought to the initial LS_1 state by thermal cycling after each laser pulse. It is worth mentioning that the experiments described in this article were conducted on many crystals of (**1**), showing very comparable and reproducible results from one crystal to another (see Figure S9).

Supporting Information
Supporting Information is available from the Wiley Online Library or from the author.

Acknowledgements
This work was supported by the European Commission through the SPINSWITCH project (H2020-MSCA-RISE-2016, Grant Agreement No. 734322).

Received: ((will be filled in by the editorial staff))
Revised: ((will be filled in by the editorial staff))
Published online: ((will be filled in by the editorial staff))

[1] K. Nasu, *Photoinduced Phase Transitions*, World Scientific, **2004**.

[2] S. Koshihara, Y. Tokura, K. Takeda, T. Koda, *Phys. Rev. Lett.* **1992**, *68*, 1148.

[3] M. Chollet, L. Guerin, N. Uchida, S. Fukaya, H. Shimoda, T. Ishikawa, K. Matsuda, T. Hasegawa, A. Ota, H. Yamochi, G. Saito, R. Tazaki, S. Adachi, S. Koshihara, *Science* **2005**, *307*, 86.

[4] M. Gao, C. Lu, H. Jean-Ruel, L. C. Liu, A. Marx, K. Onda, S. Koshihara, Y. Nakano, X. Shao, T. Hiramatsu, G. Saito, H. Yamochi, R. R. Cooney, G. Moriena, G. Sciaini, R. J. D. Miller, *Nature* **2013**, *496*, 343.

[5] P. Beaud, A. Caviezel, S. O. Mariager, L. Rettig, G. Ingold, C. Dornes, S.-W. Huang, J. A. Johnson, M. Radovic, T. Huber, T. Kubacka, A. Ferrer, H. T. Lemke, M. Chollet, D. Zhu, J. M. Glownia, M. Sikorski, A. Robert, H. Wadati, M. Nakamura, M. Kawasaki, Y. Tokura, S. L. Johnson, U. Staub, *Nat. Mater.* **2014**, *13*, 923.

[6] T. Ishikawa, S. A. Hayes, S. Keskin, G. Corthey, M. Hada, K. Pichugin, A. Marx, J. Hirscht, K. Shionuma, K. Onda, Y. Okimoto, S. Koshihara, T. Yamamoto, H. Cui, M. Nomura, Y. Oshima, M. Abdel-Jawad, R. Kato, R. J. D. Miller, *Science* **2015**, *350*, 1501.

[7] J. K. Behera, X. Zhou, J. Tominaga, R. E. Simpson, *Opt. Mater. Express* **2017**, *7*, 3741.

[8] A. Cavalleri, Cs. Tóth, C. W. Siders, J. A. Squier, F. Ráksi, P. Forget, J. C. Kieffer, *Phys. Rev. Lett.* **2001**, *87*, 237401.

[9] A. Cavalleri, *Contemp. Phys.* **2018**, *59*, 31.

[10] A. Kirilyuk, A. V. Kimel, T. Rasing, *Rev. Mod. Phys.* **2010**, *82*, 2731.

[11] P. Gütlich, A. Hauser, H. Spiering, *Angew. Chem. Int. Ed.* **1994**, *33*, 2024.

[12] P. Gütlich, H. A. Goodwin, *Spin Crossover in Transition Metal Compounds I-III*, Springer-Verlag, Berlin, Heidelberg, **2004**.

[13] A. Bousseksou, G. Molnár, L. Salmon, W. Nicolazzi, *Chem. Soc. Rev.* **2011**, *40*, 3313.

[14] A. Hauser, in *Spin Crossover in Transition Metal Compounds II* (Eds: P. Gütlich, H. A. Goodwin), Springer-Verlag, Berlin, Heidelberg, **2004**, pp. 155–198.

[15] J. K. McCusker, K. N. Walda, R. C. Dunn, J. D. Simon, D. Magde, D. N. Hendrickson, *J. Am. Chem. Soc.* **1992**, *114*, 6919.

[16] C. Bressler, C. Milne, V.-T. Pham, A. ElNahhas, R. M. van der Veen, W. Gawelda, S. Johnson, P. Beaud, D. Grolimund, M. Kaiser, C. N. Borca, G. Ingold, R. Abela, M. Chergui, *Science* **2009**, *323*, 489.

[17] A. Cannizzo, C. J. Milne, C. Consani, W. Gawelda, Ch. Bressler, F. van Mourik, M. Chergui, *Coord. Chem. Rev.* **2010**, *254*, 2677.

[18] W. Zhang, R. Alonso-Mori, U. Bergmann, C. Bressler, M. Chollet, A. Galler, W. Gawelda, R. G. Hadt, R. W. Hartsock, T. Kroll, K. S. Kjær, K. Kubiček, H. T. Lemke, H. W. Liang, D. A. Meyer, M. M. Nielsen, C. Purser, J. S. Robinson, E. I. Solomon, Z. Sun, D. Sokaras, T. B. van Driel, G. Vankó, T.-C. Weng, D. Zhu, K. J. Gaffney, *Nature* **2014**, *509*, 345.

[19] G. Auböck, M. Chergui, *Nat. Chem.* **2015**, *7*, 629.

[20] H. T. Lemke, K. S. Kjær, R. Hartsock, T. B. van Driel, M. Chollet, J. M. Glownia, S. Song, D. Zhu, E. Pace, S. F. Matar, M. M. Nielsen, M. Benfatto, K. J. Gaffney, E. Collet, M. Cammarata, *Nat. Commun.* **2017**, *8*, 15342.

[21] M. Lorenc, J. Hébert, N. Moisan, E. Trzop, M. Servol, M. Buron-Le Cointe, H. Cailleau, M. L. Boillot, E. Pontecorvo, M. Wulff, S. Koshihara, E. Collet, *Phys. Rev. Lett.* **2009**, *103*, 028301.

[22] M. Lorenc, Ch. Balde, W. Kaszub, A. Tissot, N. Moisan, M. Servol, M. Buron-Le Cointe, H. Cailleau, P. Chasle, P. Czarnecki, M. L. Boillot, E. Collet, *Phys. Rev. B* **2012**, *85*, 054302.

[23] R. Bertoni, M. Lorenc, A. Tissot, M.-L. Boillot, E. Collet, *Coord. Chem. Rev.* **2015**, *282–283*, 66.

[24] R. Bertoni, M. Lorenc, T. Graber, R. Henning, K. Moffat, J.-F. Létard, E. Collet, *CrystEngComm* **2016**, *18*, 7269.

[25] R. Bertoni, M. Lorenc, H. Cailleau, A. Tissot, J. Laisney, M.-L. Boillot, L. Stoleriu, A. Stancu, C. Enachescu, E. Collet, *Nat. Mater.* **2016**, *15*, 606.

[26] R. Bertoni, E. Collet, H. Cailleau, M.-L. Boillot, A. Tissot, J. Laisney, C. Enachescu, M. Lorenc, *Phys. Chem. Chem. Phys.* **2019**, *21*, 6606.

[27] K. Ridier, A.-C. Bas, V. Shalabaeva, W. Nicolazzi, L. Salmon, G. Molnár, A. Bousseksou, M. Lorenc, R. Bertoni, E. Collet, H. Cailleau, *Adv. Mater.* **2019**, *31*, 1901361.

[28] H. Spiering, in *Spin Crossover in Transition Metal Compounds III* (Eds: P. Gütlich, H. A. Goodwin), Springer-Verlag, Berlin, Heidelberg, **2004**, pp. 171–195.

[29] K. Ridier, G. Molnár, L. Salmon, W. Nicolazzi, A. Bousseksou, *Solid State Sci.* **2017**, *74*, A1.

[30] E. Freysz, S. Montant, S. Létard, J.-F. Létard, *Chem. Phys. Lett.* **2004**, *394*, 318.

[31] H. Liu, A. Fujishima, O. Sato, *Appl. Phys. Lett.* **2005**, *86*, 122511.

[32] S. Bonhommeau, G. Molnár, A. Galet, A. Zwick, J.-A. Real, J. J. McGarvey, A. Bousseksou, *Angew. Chem. Int. Ed.* **2005**, *44*, 4069.

[33] S. Cobo, D. Ostrovskii, S. Bonhommeau, L. Vendier, G. Molnár, L. Salmon, K. Tanaka, A. Bousseksou, *J. Am. Chem. Soc.* **2008**, *130*, 9019.

[34] G. Galle, J. Degert, C. Mauriac, C. Etrillard, J. F. Letard, E. Freysz, *Chem. Phys. Lett.* **2010**, *500*, 18.

[35] G. Gallé, D. Deldicque, J. Degert, Th. Forestier, J.-F. Létard, E. Freysz, *Appl. Phys. Lett.* **2010**, *96*, 041907.

[36] S. Bedoui, M. Lopes, W. Nicolazzi, S. Bonnet, S. Zheng, G. Molnár, A. Bousseksou, *Phys. Rev. Lett.* **2012**, *109*, 135702.

[37] G. Gallé, C. Etrillard, J. Degert, F. Guillaume, J.-F. Létard, E. Freysz, *Appl. Phys. Lett.* **2013**, *102*, 063302.

[38] M. Castro, O. Roubeau, L. Piñeiro-López, J. A. Real, J. A. Rodríguez-Velamazán, *J. Phys. Chem. C* **2015**, *119*, 17334.

[39] E. Collet, L. Henry, L. Piñeiro-López, L. Toupet, J. A. Real, *Curr. Inorg. Chem.* **2016**, *6*, 61.

[40] H. W. Liu, K. Matsuda, Z. Z. Gu, K. Takahashi, A. L. Cui, R. Nakajima, A. Fujishima, O. Sato, *Phys. Rev. Lett.* **2003**, *90*, 167403.

[41] H. Matsuzaki, T. Matsuoka, H. Kishida, K. Takizawa, H. Miyasaka, K. Sugiura, M. Yamashita, H. Okamoto, *Phys. Rev. Lett.* **2003**, *90*, 046401.

[42] K. Ridier, A.-C. Bas, Y. Zhang, L. Routaboul, L. Salmon, G. Molnár, C. Bergaud, A. Bousseksou, *Nat. Commun.* **2020**, *11*, 3611.

[43] K. Ridier, S. Rat, H. J. Shepherd, L. Salmon, W. Nicolazzi, G. Molnár, A. Bousseksou, *Phys. Rev. B* **2017**, *96*, 134106.

[44] S. Rat, K. Ridier, L. Vendier, G. Molnár, L. Salmon, A. Bousseksou, *CrystEngComm* **2017**, *19*, 3271.

[45] K. Ridier, S. Rat, L. Salmon, W. Nicolazzi, G. Molnár, A. Bousseksou, *Phys. Chem. Chem. Phys.* **2018**, *20*, 9139.

[46] C. P. Slichter, H. G. Drickamer, *J. Chem. Phys.* **1972**, *56*, 2142.

[47] A. Hauser, *J. Chem. Phys.* **1991**, *94*, 2741.

[48] K. Ridier, Y. Zhang, M. Piedrahita-Bello, C. M. Quintero, L. Salmon, G. Molnár, C. Bergaud, A. Bousseksou, *Adv. Mater.* **2020**, *32*, 2000987.

[49] C. N. R. Rao, K. J. Rao, *Phase Transitions in Solids*, McGraw Hill Book Co., **1978**.

[50] S. Liu, K. Zhou, T. Yuan, W. Lei, H.-Y. Chen, X. Wang, W. Wang, *J. Am. Chem. Soc.* **2020**, *142*, 15852.

[51] K. Bairagi, O. Iasco, A. Bellec, A. Kartsev, D. Li, J. Lagoute, C. Chacon, Y. Girard, S. Rousset, F. Miserque, Y. J. Dappe, A. Smogunov, C. Barreteau, M.-L. Boillot, T. Mallah, V. Repain, *Nat. Commun.* **2016**, *7*, 12212.

[52] V. Shalabaeva, A.-C. Bas, M. Piedrahita-Bello, K. Ridier, L. Salmon, C. Thibault, W. Nicolazzi, G. Molnár, A. Bousseksou, *Small* **2019**, *15*, 1903892.

[53] M. Gruber, R. Berndt, *Magnetochemistry* **2020**, *6*, 35.

Taking advantage of an exceptionally reversible bidirectional switching in a molecular spin-crossover crystal, pump-probe optical microscopy is used to explore the dynamics of the spin-state switching within the bistability region. The movies of the photo-induced domino effect reveal that the proliferation of the photo-induced phase is delayed successively by the molecular and the thermodynamic energy barriers, leading to two successive self-amplification steps on sub-µs and ms timescales, respectively.

K. Ridier*, W. Nicolazzi, L. Salmon, G. Molnár* and A. Bousseksou*

Sequential activation of molecular and macroscopic spin-state switching within the hysteretic region following pulsed light excitation